

**Investigations of “Mesa” Beams for LIGO**

D. Zeb Rocklin

LIGO Laboratory, California Institute of Technology, Pasadena, CA 91125 USA

**ABSTRACT**

Mirror thermal noise is one of the limiting factors in the sensitivity of current and future gravitational wave observatories including Advanced LIGO. Non-Gaussian beam profiles such as the flat-topped “mesa” beam can be employed in gravitational wave interferometers to reduce the effect of this noise. Mesa beams are generated in a Fabry-Perot cavity by replacing the baseline spherical mirrors with “Mexican Hat” (MH) mirrors which have a different profile. MH cavities differ from traditional cavities in both theoretical and practical ways. MH cavities are a few times more sensitive to tilt, causing increased coupling to higher-order modes that reduces the sensitivity of the device. We use wavefront sensing to demonstrate an error signal that can be used to measure the alignment of the cavity. This technique is vital for automatic cavity alignment.

**TEXT:**

The Laser Interferometer Gravitational Wave Observatory (LIGO) is dedicated to the detection of gravitational waves. Because general relativity predicts that even the most powerful of cosmological events will change the lengths of the interferometer arms by only about one part in  $10^{22}$ , the instrument has to be extremely precise<sup>1</sup>. Using mesa beams in place of the normal Gaussian beam profile can significantly increase the instrument’s sensitivity<sup>2</sup>.

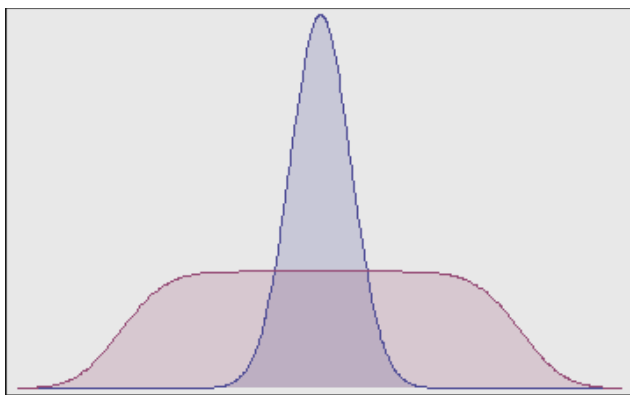


LIGO’s site in Livingston, LA. Its two 4km arms contain Fabry-Perot cavities in which laser light resonates. The interference pattern between the light from the two arms can measure small changes in arm length, such as those caused by gravitational waves, very precisely.

LIGO works by creating an interference pattern between two parts of a laser beam that is split and fired through two interferometer arms. The device is adjusted so that when no gravitational waves are present the beams interfere perfectly destructively at the dark port detector, producing no signal. When a gravitational wave passes through the detector, or any of several sources generate noise, a signal is generated. While there are algorithms which can differentiate the true signal from the noise<sup>2</sup>, it is crucial that the noise sources, which are often much more powerful than the true signal, be reduced as much as possible.

The use of mesa beams in the interferometer is one of the most promising means of reducing mirror thermal noise<sup>3</sup>. Thermoelastic noise is caused by fluctuations in the mirrors' surfaces resulting from random heat flow. These fluctuations limit the ability of the beam to detect the exact position of the mirror surface. In Advanced LIGO, the much-anticipated 2011 LIGO upgrade<sup>4</sup>, thermoelastic noise will be one of the limiting factors in sensitivity<sup>5</sup>.

A mesa beam has an intensity profile of a Gaussian beam integrated around a disk. It can be thought of as very many Gaussian beams superimposed upon each other but spread out around a circular region of space. Because of its wider power distribution, a mesa beam is able better probe the position of a real mirror. Beams of arbitrary flatness can't be produced as the finite size of the mirrors produce diffraction effects that cause power loss as part of the beam "falls off" the mirror. Mesa beams manage to sample a greater percentage of the mirror without suffering prohibitive diffraction losses. One proposed mesa profile has been calculated to reduce thermoelastic noise by a factor of 2.9, with a corresponding increase in detection rates of inspiraling binaries of about 2.6<sup>3</sup>. This is the main motivation for exploring mesa beam cavities.



The mesa beam (lavender) has a much wider power distribution than the baseline Gaussian (blue) and samples a wider part of the mirror's surface.

Special mirrors must be used within the Fabry-Perot cavity to generate the mesa beam. By choosing a mirror surface which has a mesa eigenmode (if a mesa beam is incident, the same beam profile is reflected) one can create a cavity in which mesa beams resonate. Then, although a Gaussian beam is incident upon the cavity, the mesa mode resonates in the cavity, with the remaining portions of the incident beam being rejected by the cavity. It is still important to choose a Gaussian beam with as great an overlap with the mesa mode as possible. In fact this overlap is quite large—as high as 94%<sup>5</sup>. This

large overlap is very important for the practical implementation of mesa beam cavities.

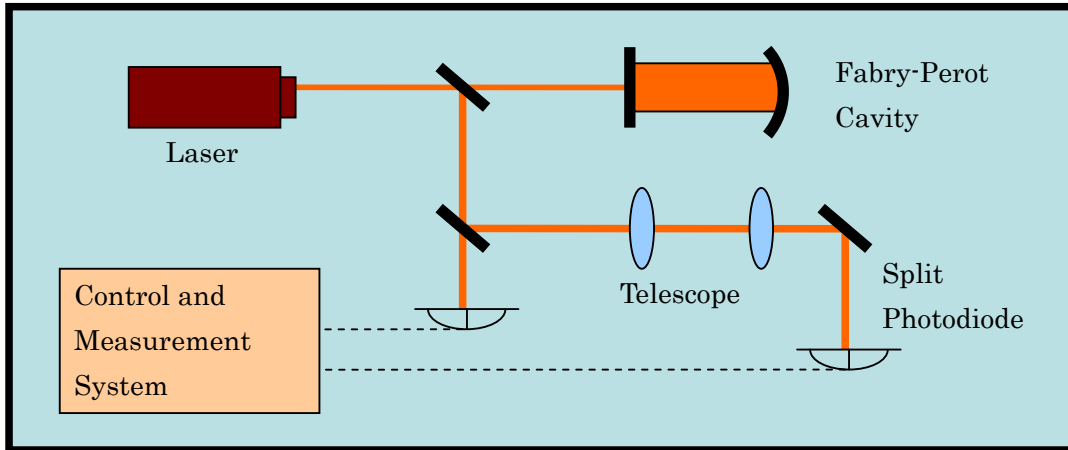
Despite mesa beams' superior thermal properties, implementing a new mirror profile inevitably raises new concerns and requires the modification of standard techniques. One major concern is cavity misalignment. The cavity can become misaligned in any of several ways: either of the mirrors can be displaced in either lateral direction, or tilted about two axes, or the mirrors' physical parameters might not match in certain ways. Of these, the most concerning in practice is expected to be mirror tilt, which can reduce device sensitivity. While this is true of both baseline and mesa cavities, it is expected that mesa cavities will be somewhat more sensitive to tilt.

We develop a mathematical framework to describe mirror tilt and describe a sensing scheme to measure the alignment of a cavity using a technique known as *wavefront sensing*. Through simulation, we find an error signal that determines both the magnitude and the direction of tilt. Such a signal can be integrated with a control system to allow automatic cavity alignment<sup>6</sup>.

When a cavity mirror becomes tilted, it couples the base mode of the cavity to higher-order modes. This changes the shape of the field that exits the Fabry-Perot cavity and is incident upon the detectors. Using these detectors to determine the shape of the beam is what gives wavefront sensing its name—by determining the beam's shape, the alignment of the cavity can be measured very precisely.

The key difference between the base mesa mode and the first excited mode is the latter's asymmetry. Because of this, if one takes a split photodiode and subtracts the power incident on one half from that on the other, one can measure the amount of first-order mode present. If one takes a quadrant photodiode, one can measure excited modes from tilts in both directions. It is from this method, which measures not just the size but the shape of the beam, that wavefront sensing takes its name.

However, both mirror tilt and mirror offset couple to the same higher-order modes. Additional measures are necessary to discern between them. The Guoy phase telescope consists of a series of lenses designed to shift the Guoy phase—the phase difference between the Gaussian beam and a plane wave—some amount. It is also important for controlling the width of the beam. If the beam is too wide most of it will fall off the photodiode and if it is too narrow it is difficult to align the photodiode's center with that of the beam. The mode contribution of mirror tilt is  $90^\circ$  out of phase with that of mirror offset. Passing through the telescope adds  $90^\circ$  of phase to the base mode and  $180^\circ$  to the excited modes from tilt and offset. The telescope puts excited mode generated by mirror offset in phase with the base mode and moves that generated by mirror tilt out of phase with it. Thus, prior to the mirror, a split photodiode can strongly detect mirror tilt, and is blind to mirror offset. After the telescope, the reverse is true.



In wavefront sensing, the misalignment of the Fabry-Perot cavity is determined by measuring and quantifying the shape of the leakage beam from the cavity. Split photodiodes are employed to measure the asymmetric character of the beam (quadrant photodiodes for x and y directions). Multiple sensors, including photodiodes before and after a Guoy Phase Telescope, combine to produce a multi-dimensional error signal that can measure many different types of misalignment simultaneously. Ultimately, such a measurement can be attached to cavity controls as a method of automatic cavity alignment.

One of the experimental difficulties in wavefront sensing is the placement of detectors and the configuration of the telescope that makes each detector sensitive most strongly to only one mode. Mathematically, this corresponds to adjusting the apparatus to produce a matrix relating error signals to misalignments that is as nearly diagonal as possible. While for Gaussian beams good agreement between calculations and experiment has been found<sup>7</sup> the lack of an analytic expression for the Guoy phase of mesa modes complicates matters somewhat in our case.

Due to unforeseeable difficulties in lab availability, the experimental production of the wavefront sensing has not been realized. We intend to complete this portion of the work as soon as the lab becomes available.

However, the wavefront sensing apparatus has been implemented in simulation (see methods) and error signals such as those needed for an automatic alignment system have been generated. Important parameters such as the strength of the signal and its linear regime have been determined. The realization of wavefront sensing for non-Gaussian beams encourages the study of implementing novel beam profiles such as are being investigated<sup>8,9</sup>. The generation of an error signal serves as an important test of future experimental work. Most importantly, however, the work demonstrates the practicality of mesa beams, which are still being considered as an option for AdvLIGO.

## METHODS:

**Mesa Beam Cavities:**

The mesa beam cavity is driven by a Gaussian beam with a similar shape. The mesa beam profile is given by

$$\text{Mesa } (x, y, z, D) = e^{i k z} e^{-i \tan^{-1} (z/z_0)} \int_{x_0^2 + y_0^2 \leq D^2} \exp \left[ \frac{((x-x_0)^2 + (y-y_0)^2) (1 - i z / z_0)}{2 \sqrt{\frac{z_0}{k}} \sqrt{1 + \left(\frac{z}{z_0}\right)^2}} \right] dA_0$$

$(x_0, y_0)$  : The center of the beam in the cross section.

$z_0$ :  $\pi w_0^2 / \lambda$  ( $w_0$  is the characteristic length of the Gaussian at the beam's waist, its narrowest cross section)

$k$  : the wavenumber,  $2\pi/\lambda$

$D$ : the radius of the disk over which the Gaussian beam is integrated

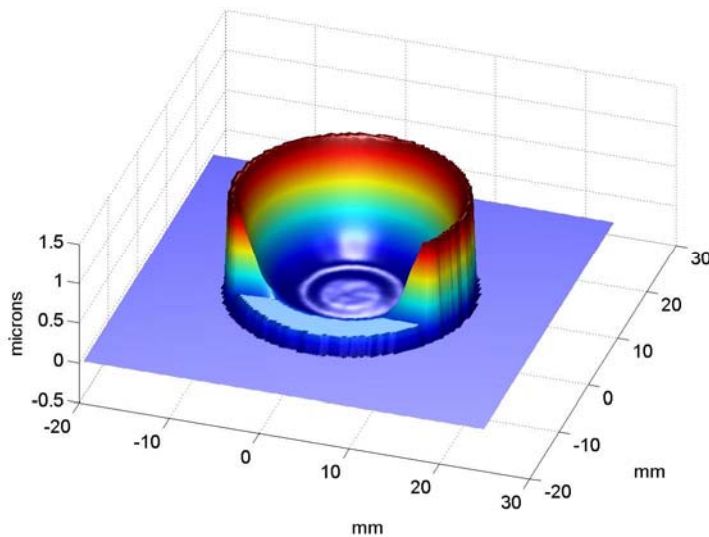
The general eigencondition for a cavity is that the mirrors have profiles so that the propagation phase accumulated at any point on the wavefront is equal to its relative phase:

$$k h (r) = \text{Arg}[ U_{\text{mesa}} (r) ]$$

It is this requirement that produces the “Mexican Hat” shape. Like all finite-sized mirrors, some fraction of the power is lost through diffraction. The properly-aligned cavity has a diffraction loss of 11.40 Parts Per Million (ppm).

**Mirror Production:**

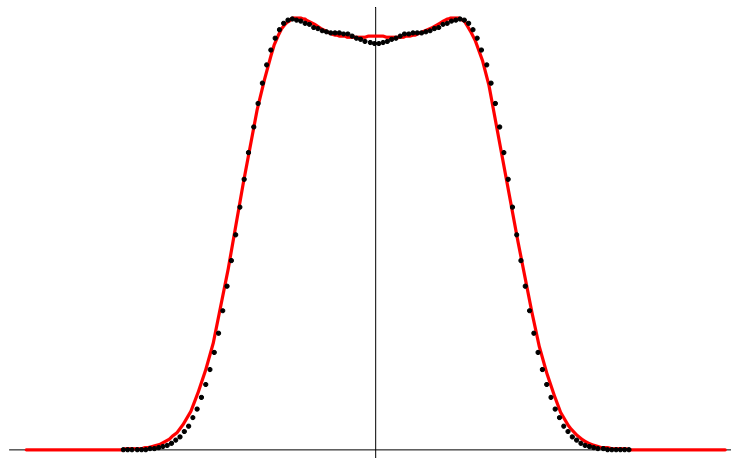
The mirrors are created through a three-step process<sup>10</sup>. In all steps, an ion beam causes silica atoms to be emitted through a screen onto the micro-polished mirror substrate. In the first step, a “mask” with the MH profile is cut in the screen and the substrate is rotated as the profile is applied with a 60 nm Peak-to-Valley (PV) precision. In the second step, the process is repeated slowly, to achieve a 10 nm PV precision. In the third step, interferometry is used to measure the deposition error and the position of the substrate is automatically adjusted to correct the error. The method is very good at achieving arbitrary mirror profiles. However, it can be a lengthy process and cannot achieve slopes of greater than 500 nm/ mm. However, note that the eigencondition requires very flat mirrors, with total heights on the order of the wavelength (1064 nm) for total diameters on the order of the beam width (centimeters).



This false-color scan of the real MH mirror's surface was created using a computer interferometry scan. The mirrors create a cavity with the desired mesa beam as the eigenmode.

***Fast Fourier Transform Simulation:***

The principal tool I used to investigate the properties of a realistic, misaligned cavity was a Fast Fourier Transform (FFT) simulation developed by Hiro Yamamoto. FFT simulations are a fast and accurate way of simulating real optical cavities<sup>11</sup>.



The distribution of power in the cavity (at the ITM). The results from the FFT simulation (black points) recover the theoretical shape (red line).

***Modal Model:***

Following the formalism associated with Gaussian beams<sup>15</sup>, one typically describes the results of cavity misalignment in terms of “higher-order modes”. While one has an infinite number of families of modes one could choose, higher-order Gaussians are typically decomposed in terms of the Hermite-Gauss or Laguerre-Gauss bases. The former of the two has the virtue of describing the results of small tilts as

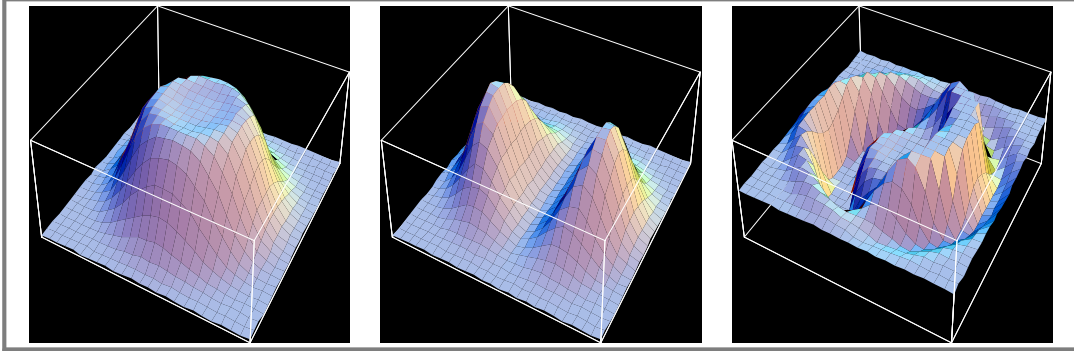
first-order corrections. Motivated by this, I searched for an analogous basis to describe misaligned mesa cavities. We suppose that a higher-order mode consists of:

$M_{nm}(x,y) = u_n(x)u_m(y)M(x,y)$ , with  $u_i$  being an  $i^{\text{th}}$ -order polynomial and  $M(x,y)$  the base mesa mode. By imposing a standard orthonormality requirement I was able to generate the entire basis of orthonormal modes:

$$\langle u_n u_m | u_i u_j \rangle \equiv \iint u_n(x) u_m(y) u_i^*(x) u_j^*(y) dx dy = \delta_{ni} \delta_{mj}$$

Where  $\delta$  denotes the Kronecker delta.

These requirements along with the base mode suffice to generate the entire basis. Unlike the Hermite-Gaussian polynomials, which have integer polynomial coefficients, the coefficients of the Mesa basis are non-analytical. In fact, any rotationally symmetric beam can be used to generate a similar basis. One can easily see that orthogonality requires each mode polynomial to contain only even or odd terms. The results from the simulation confirm that to first order in a tilt of the rear mirror (End Test Mass or ETM) the first-order mode defined this way is the only one excited. Our analysis expands the field in terms of the first five modes as tilt ranges up to 400 nanoradians, which accounts for 99.65% of the power.

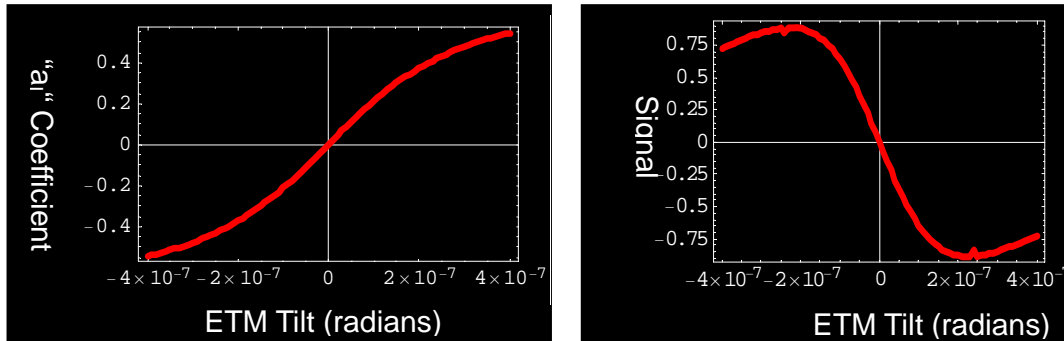


From a field  $a_0 M_{00} + a_1 M_{01}$ , the intensity profile generated is  $|a_0 M_{00}|^2 + |a_1 M_{01}|^2 + 2 \text{Re}(a_0 a_1^* M_{00} M_{01}^*)$ . From left to right, the power distributions above are  $|M_{00}|^2$ ,  $|M_{01}|^2$ , and  $2 \text{Re}(M_{00} M_{01}^*)$ . It is the third component and only the third component of the power which is detected by a split photodiode. This signal is proportionate to  $a_1$ , which is itself proportionate to the tilt angle (for small angles).

Using the basis modes, the coefficients of the field within the cavity can very easily be calculated. If the total field is  $E(r) = \sum a_i M_i(r)$ , then each coefficient  $a_i$  is simply  $\langle E | M_i \rangle$ . The first two coefficients measured from the simulation,  $a_1 = 2.25 \cdot 10^6 \text{ rad}^{-1}$  and  $a_2 = 1.67 \cdot 10^{12} \text{ rad}^{-2}$  comparing very well with the previously-reported values of  $2.27 \cdot 10^6$  and  $1.8 \cdot 10^{12}$  respectively<sup>2</sup>.

However, of course the field within a physical cavity is not directly measurable in a physical apparatus. Instead, detectors are placed to detect the field reflected from the cavity. The key term, especially for small tilts, is the  $2 \text{Re}(M_{00}^* M_{10})$ . However, due to the orthogonality of the modes, this is

not detectable with a regular photodiode. Instead, a split photodiode is used, and the power incident on one end is subtracted from that incident on the other. In this way, only the  $2 \operatorname{Re}(M_{00}^* M_{10})$  is detected (as well as other cross-terms, negligible at small angles). Using the simulation, I was able to produce the following error signal:

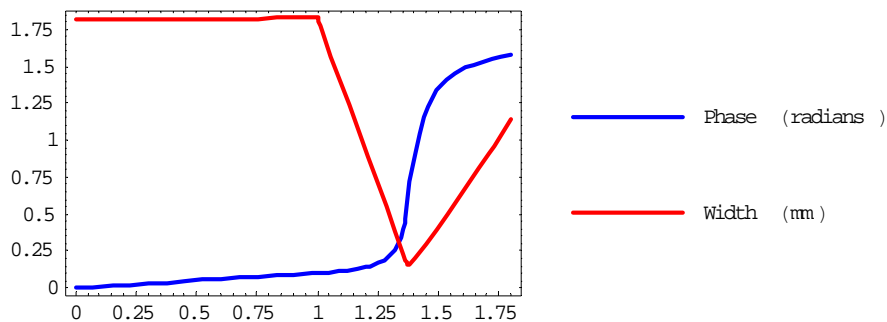


The modal model is extremely useful for understanding the error signal resulting from misalignment. In particular, the departure from linearity and even monotonicity can be explained in terms of the increasing second-order effects. The second-order mode couples to the base mode with opposite phase of the first-order mode. Note that this is with respect to the antisymmetric kernel of the split photodiode: the modes are orthogonal, and thus their cross-term is invisible to a regular photodiode.

### Guoy Phase Telescope:

The Guoy phase telescope is a series of focusing lenses that moves the beam from the near-field to the far-field regime. Hermite-Gaussian modes acquire an amount of Guoy phase equal to<sup>12</sup>:

$$\Phi = (m + n + 1) \arctan(z / z_0)$$

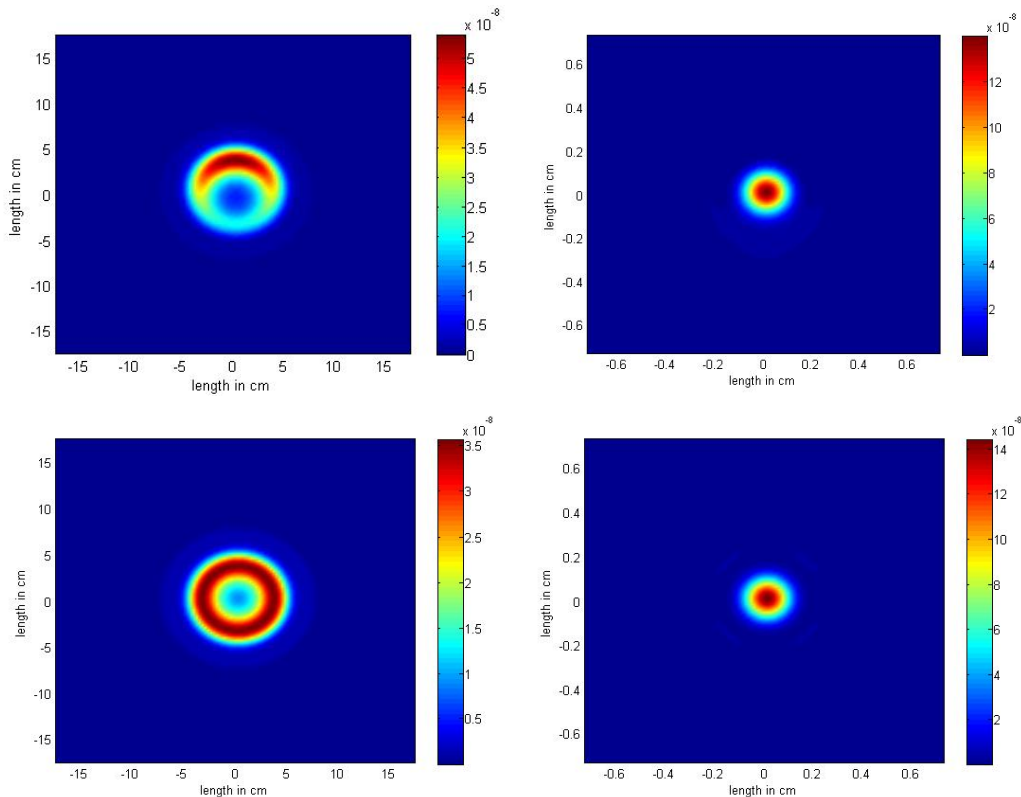


I wrote a simple program to analytically describe the effect of a GPT on a Gaussian beam. Above, a series of two mirrors located at distances of 1 and 1.372 meters from the beam waist takes an input Gaussian beam through a phase change of  $90^\circ$  while reducing the width of the beam. The focal lengths of the mirrors correspond to commercially available lenses, and the Guoy Phase Telescope fits within an 80 cm area, and so may be used with our laboratory apparatus. The control a GPT exerts over the beam width is also important, as if it is too large, it may fall off the photodiodes, and if it is too small, it becomes difficult to align the photodiodes.



Recall that the error signal is proportionate to  $\text{Re}(a_0 a_1^*)$ . As such, the phase between the two modes controls the strength of the signal. Because different modes acquire different amounts of phase, the error signal can be adjusted by propagating the beam through the telescope. In fact, the higher-order modes generated by offset mirrors are out of phase with the base mode, and those generated by mirror tilt are in-phase. As such, the error signal measured before the GPT emphasizes mirror tilt, while that measured after emphasizes mirror offset. However, with the GPT used, the signal for a reasonable offset was still much smaller than that caused by tilt. Previous wavefront-sensing experiments have also reported difficulty in detecting offset<sup>12</sup>.

	Near Field Error Signal	Far Field Error Signal
Offset Mirror ( $4 \cdot 10^{-6}$ meters)	$-2.46033 \cdot 10^{-8}$	$-1.25389 \cdot 10^{-7}$
Tilted Mirror ( $4 \cdot 10^{-8}$ rad )	$-.297871$	.0845955



Upper Left: The field exiting the Fabry-Perot cavity with the ETM tilted by  $4 \cdot 10^{-8}$  radians. Upper Right: The field after being propagated through a GPT. Its first-order mode has moved out of phase with the base mesa mode, which now dominates. Lower Left: The field exiting a Fabry-Perot cavity with the ETM offset by 4 microns. Lower Right: the same field, propagated through a GPT. The presence of the first-order mode is too slight to be observed on the lower graphs, despite its magnification

by the GPT.

#### **ACKNOWLEDGEMENTS:**

This work was supported by the California Institute of Technology Summer Undergraduate Research Fellowship (SURF) program and administered through the Laser Interferometer Gravitational-Wave Observatory (LIGO) with funds from the National Science Foundation's (NSF) Research Experience for Undergraduates (REU) program.

In addition to my faculty mentors, John Miller and Riccardo DeSalvo, I would like to thank Hiro Yamamoto for helpful discussions regarding his FFT simulation.

#### **REFERENCES:**

- [1] A. Abramovici et al "Ligo: The laser interferometer gravitational-wave observatory," *Science* **256**, pp. 325-333, 1992
  
- [2] B. Owen, B. Sathyaprakash, "Matched filtering of gravitational waves from inspiraling compact binaries: Computational cost and template placement," *Phys. Rev. D* **60**, (1999)
  
- [3] E. D'Ambrosio, R. O'Shaughnessy, S. Strigin, K. S. Thorne, S. Vyatchanin, "Status Report on Mexican-Hat Flat-Topped Beams for Advanced LIGO," LIGO Report No. T030009-00-R (2003).
  
- [4] <http://www.ligo.caltech.edu/advLIGO/>
  
- [5] E. D'Ambrosio, R. O'Shaughnessy, S. Strigin, K. S. Thorne, S. Vyatchanin, "Reducing Thermoelastic Noise in Gravitational-Wave Interferometers by Flattening the Light Beams," (forthcoming, available at [http://admdbsrv.ligo.caltech.edu/lsc\\_papers/default\\_reviewed.htf](http://admdbsrv.ligo.caltech.edu/lsc_papers/default_reviewed.htf)).
  
- [6] E. Morrison, B. J. Meers, D. I. Robertson, H. Ward, "Automatic alignment of optical interferometers," *Appl. Opt.* **33**, (1994).
  
- [7] N. Mavalvala, "Alignment Issues in Laser Interferometric Gravitational-Wave Detectors," Ph.D. thesis, MIT, 1990.
  
- [8] Pierro, Galdi, Castaldi, Pinto, Agresti, DeSalvo, "Perspectives on Beam-Shaping Optimization for Thermal-Noise Reduction in Advanced Gravitational-Wave Interferometric Detectors: Bounds, Profiles, and Critical Parameters"

LIGO Report No. P070066-01-Z

[9] M. Bondarescu, K. Thorne “New family of light beams and mirror shapes for future LIGO interferometers,” *Phys. Rev. D* **74** (2006)

[10] J. Agresti, E. D’Ambrosio, R. DeSalvo, J. Mackowski, A. Remilleux, B. Simoni, M. Tarallo, P. Willems “Flat top beam profile cavity prototype” LIGO Report No. P050044-00-R

[11] J-Y Vinet, P. Hello, C. N. Man, A. Brillet, “A high accuracy method for the simulation of non-ideal optical cavities,” *J. Phys. I France* **2**, (1992).

[12] H. Kogelnik and T. Li “Laser Beams and Resonators,” *Appl. Opt.* **5**, (1966).

[13] E. Morrison, B. J. Meers, D. I. Robertson, H. Ward, “Experimental demonstration of an automatic alignment system for optical interferometers,” *Appl. Opt.* **33**, (1994).

[14] E. D. Black “An Introduction to Pound-Drever-Hall laser frequency stabilization,” LIGO Report No. P990042-A, (2000).

[15] M. Eichenfield “Modelling [*sic*] and Commissioning the Wavefront Sensing Auto-Alignment System of a Triangular Mode Cleaner Cavity,” LIGO Report No. T030234-00-D (2003)

[16] N. Mavalvala, “IOO Mode Cleaner Wavefront Sensing Telescopes,” LIGO Report No. T970000-00-D (1997).

[17] E. D’Ambrosio, “Nonspherical mirrors to reduce thermoelastic noise in advanced gravitational wave interferometers,” *Phys. Rev. D* **67**, (2003).

[18] G. Heinzel, “Advanced optical techniques for laser-interferometric gravitational-wave detectors,” PhD. thesis, University of Hanover, 1999.

[19] D. Z. Anderson “Alignment of resonant optical cavities,” *Appl. Opt.* **23**, (1984).

[20] E. D’Ambrosio, R. O’Shaughnessy, K. S. Thorne, P. Willems, S. Strigin, S. Vyatchanin, “Advanced LIGO: non-Gaussian beams,” *Class. Quantum Grav.* **21**, (2004).

[21] N. M. Sampas, D. Z. Anderson “Stabilization of laser beam alignment to an optical resonator by heterodyne

detection of off-axis modes,” Appl. Opt. **29**, (1990).

[22] H. Kogelnik, “On the Propagation of Gaussian Beams of Light Through Lenslike Media Including those with a Loss or Gain Variation,” Appl. Opt. **4**, (1965).

[23] P. T. Beyersdorf, S. Zappe, M. M. Fejer, M Burkhardt, “Cavity with a deformable mirror for tailoring the shape of the eigenmode,” (forthcoming)

[24] J-Y Vinet, “Mirror thermal noise in flat-beam cavities for advanced gravitational wave interferometers,” Class. Quantum Grav. **22**, (2005).

[25] B. Simoni, “Design and Construction of a Suspended Fabry-Perot Cavity for Gaussian and Non-Gaussian Beam Testing. Preliminary Test with Gaussian Beam,” Ph.D. thesis, Universita di Pisa, 2004.

[26] M. G. Tarallo, “Experimental study of a non-gaussian [*sic*] Fabry-Perot resonator to depress mirror thermal noise for gravitational waves detectors,” Ph.D. thesis., Universita di Pisa, 2005.

[27] R. C. Lawrence, “Active Wavefront Correction in Laser Interferometric Gravitational Wave Detectors,” Ph.D. thesis, MIT, 2003

[28] D. Kennefick, “Traveling at the Speed of Thought: Einstein and the Quest for Gravitational Waves,” (Princeton University Press, 2007).

[29] H. Yamamoto “SIS (Stationary Interferometer Simulation) manual,” LIGO Report No. T070039-00-E (2007)

[30] M. J. Lawrence, B. Willke, M. E. Husman, E. K. Gustafson, R. L. Byer, “Dynamic Response of a Fabry-Perot interferometer” J. Opt. Soc. Am. B **16** (1999)

[31] E. D’Ambrosio, A. M. Gretarsson, V. Frolov, B. O’Reilly, P. K. Fritschel “Effects of mode degeneracy in the LIGO Livingston Observatory recycling cavity,” LIGO Report No. P070044-00 (2007)